Journal of Solid State Chemistry 184 (2011) 2506–2515

Contents lists available at ScienceDirect

Journal of Solid State Chemistry

journal homepage: www.elsevier.com/locate/jssc

Two new zincophosphates, $(H_3NCH_2CH_2NH_3)_2[Zn(\mu\text{-}PO_4)_2]$ and $(NH_4)[(H_3N)Zn\{(\mu\text{-}PO_4)Zn\}_3]$: Crystal structures and relationships to similar open framework zinco- and aluminophospates

Ljiljana Karanović [a,*], Dejan Poleti [b], Tamara Đorđević [c], Sabina Šutović [a]

[a] Laboratory of Crystallography, Faculty of Mining and Geology, University of Belgrade, Đušina 7, 11000 Belgrade, Serbia
[b] Department of General and Inorganic Chemistry, Faculty of Technology and Metallurgy, University of Belgrade, Karnegijeva 4, 11000 Belgrade, Serbia
[c] Institut für Mineralogie und Kristallographie, Universität Wien-Geozentrum, Althanstrasse 14, A-1090 Vienna, Austria

ARTICLE INFO

Article history:
Received 27 May 2011
Received in revised form
14 July 2011
Accepted 17 July 2011
Available online 22 July 2011

Keywords:
Zincophosphate
Inorganic–organic hybrid
Open framework structure
Hydrogen bonding
Hydrothermal synthesis

ABSTRACT

Two new zincophosphates, bis(ethylenediammonim) *catena*-bis(μ-phosphato)zincate, $(H_3NCH_2CH_2NH_3)_2[Zn(\mu\text{-}PO_4)_2]$ (**1**), and ammonium ammine-tris(μ-phosphato)tetrazincate, $(NH_4)[(H_3N)Zn\{(\mu\text{-}PO_4)Zn\}_3]$ (**2**), were synthesized under hydrothermal conditions and their crystal structures were determined by single-crystal X-ray diffraction analysis. The crystal structure of **1** consists of infinite macroanionic $ZnP_2O_8^{4-}$ chains, running along the [0 0 1] direction, and diprotonated ethylenediammonium cations, H_2en^{2+}. The crystal structure of **2** is built up from ZnO_4, $Zn(NH_3)O_3$ and PO_4 vertex-sharing tetrahedra connected to form an open 3D framework. The ammonium groups, NH_4^+, are located in the channels formed by 8M-rings extending along [1 0 0]. In order to study vibrational behavior of H_2en^{2+} and NH_4^+ cations, NH_3 molecules in **1** and **2**, single-crystal Raman spectra were obtained. Structural, chemical and topological similarities to the other open framework zinco- and aluminophosphates incorporating different guest species are discussed.

1. Introduction

Zincophosphates (ZPOs) are of particular importance because of their established and potential application as adsorbents, catalysts and ion exchangers. Their crystal structures are based on various zero-, one-, two- or three-dimensional inorganic frameworks. ZPOs built up from a 3D framework of vertex-sharing ZnO_4 and PO_4 tetrahedra are of special interest for their structural relationship to polymorphs of silicate and aluminosilicate zeolites [[1–3] and references therein]. These materials, containing channels or cages in their porous structures, are of potential usefulness in many branches of technology. Therefore, the considerable attention to ZPOs having open framework structures has expanded and their compositional and structural diversity has not been fully explored.

A large number of ZPOs and other microporous materials have been synthesized in the presence of organic amines acting as a structure-directing (template), charge-compensating and/or space-filling agents. In their presence the porous structures are likely to crystallize. The incorporation of organic molecules often form inorganic–organic hybrid compounds with interesting crystal structures, physico-chemical properties and potential applications in catalysis and biology [4]. Among other organic amines, ethylenediamine (1,2-diaminoethane) containing two protonated amino groups ($-NH_3^+$) and acting as proton donor plays an important role in the synthesis of porous materials [3,5].

Recently, several ZPOs with various Zn:P ratios have been prepared by the hydrothermal method, which is proved to be effective for the synthesis of well-developed single crystals [3,6]. We have previously reported a new ZPO, $[Zn_3(H_2O)_{0.8}(NH_3)_{1.2}(PO_4)_2]$, with layered structure and Zn:P ratio of 3:2 [7]. Here we report on a new inorganic–organic hybrid (**1**) with a chain structure (Zn:P ratio of 1:2) and a novel 3D open framework structure with Zn:P ratio of 4:3 (**2**). In addition, some phosphates adopting chain structures similar to **1**, but with different guest species, are considered and compared. Besides, the structural features of a series of ZPOs with 2D or 3D frameworks and the structural relationships among them are discussed. This is focused on the ZPOs with Zn:P ratio of 4:3 and diverse guest species.

2. Experimental

2.1. Synthesis of crystals

Both investigated compounds were obtained during the study of the $SrO–ZnO–P_2O_5–NH_3–H_2O$ system and the corresponding

* Corresponding author. Fax: +381 11 2635 217.
E-mail address: ljika2002@yahoo.com (L. Karanović).

0022-4596/$ - see front matter © 2011 Elsevier Inc. All rights reserved.
doi:10.1016/j.jssc.2011.07.030

four-component systems with or without structure-directing agents. The compounds were synthesized hydrothermally from starting mixtures of the following: $5ZnO \cdot 2CO_3 \cdot 4H_2O$ (Alfa Products, >99%), $(NH_4)_2HPO_4$ (Loba Chemie, >99%) in a 1:1 molar ratio and 1 ml of ethylenediamine (Alfa Aesar, 99%) for **1**, and $Sr(OH)_2 \cdot 8H_2O$ (Merck, >97%), $5ZnO \cdot 2CO_3 \cdot 4H_2O$ and $(NH_4)_2HPO_4$ in a 1:1:1 molar ratio for **2**. The mixtures were transferred into Teflon vessels and filled to approximately 70% of their volume with distilled water. The initial pH values of the mixtures were 10 and 9 for **1** and **2**, respectively. Finally, they were enclosed into stainless steel autoclaves. The mixture for **1** was heated under autogeneous pressure to 160 °C, held at this temperature for 72 h and cooled to room temperature over a period of 96 h. The pH of supernatant solution was 9. The mixture for **2** was heated under autogeneous pressure at 200 °C for 9 days and spontaneously cooled to room temperature. The resulting products were filtered, washed thoroughly with distilled water and dried in air at room temperature. The compound **1** was crystallized as prismatic colorless transparent crystals (yield about 50%), while the compound **2** was crystallized as a needle-like colorless transparent crystals (yield about 30%) of up to 0.8 and 0.4 mm in length, respectively, together with uninvestigated white powder.

2.2. Crystal data collection, refinement and Raman spectra

A suitable crystal of **1** was selected for the X-ray structure analysis. X-ray measurement was done on an Oxford Xcalibur Gemini diffractometer equipped with a Sapphire3 CCD detector. The X-ray data were collected at room temperature using graphite-monochromatized Mo$K\alpha$ radiation and ω scans. Unit cell parameters were determined by least squares on the basis of 2171 reflections. Data integration and scaling of the reflections were performed with the CrysAlisPro suite [8]. Empirical absorption correction (multi-scan) was applied using spherical harmonics, implemented in SCALE3 ABSPACK scaling algorithm [8].

The room temperature intensity data of **2** were collected on a Nonius Kappa CCD single-crystal four-circle diffractometer (Mo$K\alpha$ radiation, graphite monochromator), equipped with a 300 mm diameter capillary-optics collimator. Unit cell parameters were determined by least square refinement based on 5939 reflections with HKL SCALEPACK [9]. A complete sphere of reciprocal space (φ and ω scans) was measured. The intensity data were processed with the Nonius program suite DENZO-SMN [9] and corrected for absorption by the multi-scan method [9,10].

Both structures were solved by direct methods [11] and refined on F^2 by full-matrix least-squares using SHELXL97 [12] and WinGX [13]. All non-hydrogen atoms were refined anisotropically. All H atoms were placed in geometrically ideal positions and were refined using the riding model, with fixed atomic displacement parameters $U_{iso}(H)=1.2\ U_{eq}(N)$ or $1.2\ U_{eq}(C)$. Both, NH_4^+ cation and NH_3 molecules, were refined as rigid groups keeping the interatomic distances and angles fixed. The C–H distances from methylene groups and N–H distances were constrained to 0.97 and 0.89 Å, respectively. Selected crystal and experimental data are given in Table 1. The final atomic coordinates and anisotropic displacement parameters are given in Supplementary material (Tables S1 and S2). The selected bond distances and bond angles are listed in Table 2, and hydrogen bonding geometry in Table 3. All drawings were produced with ATOMS [14].

In order to study spectral properties of **1** and **2**, single-crystal Raman spectra of randomly orientated crystals were obtained by means of a dispersive Horiba Jobin–Yvon LabRam–HR system in the spectroscopic range from 4000 to 80 cm^{-1} for **1** and 4000 to 100 cm^{-1} for **2**. This spectrometer has a focal length of 800 mm and it equipped with an Olympus BX41 optical microscope, a

Table 1
Crystal data, data collection and refinement details for **1** and **2**.

Crystal data	**1**	**2**
Chemical formula	$C_4H_{20}N_4O_8P_2Zn$	$H_3NO_{12}P_3Zn_4 \cdot H_4N$
Temperature (K)	295(2)	293(2)
Formula weight, M_r (g mol^{-1})	379.57	581.47
System, space group (no.)	Orthorhombic, *Pccn* (56)	Triclinic, $P\bar{1}$(2)
a (Å)	17.2060(3)	5.1896(10)
b (Å)	8.4950(7)	8.0221(16)
c (Å)	8.7840(3)	15.905(3)
α (°)	90	94.29(3)
β (°)	90	92.24(3)
γ (°)	90	108.58(3)
V (Å^3)	1283.91(11)	624.5(2)
Z	4	2
F(0 0 0)	784	564
Calculated density D_x (g cm^{-3})	1.964	3.092
Absorption coefficient, μ (mm^{-1})	2.21	8.04
Transmission factors, T_{min}/T_{max}	0.4725/0.6668	0.1413/0.5003
Crystal size (mm)	0.4 × 0.2 × 0.2	0.4 × 0.1 × 0.1
Reflections collected/unique	3173/1312	15289/2749
Observed reflections [$I > 2\ \sigma(I)$]	1110	2430
R_{int}	0.019	0.033
Range for data collection, θ (°)	3.54–26.36	1.29–27.10
Range of Miller indices	$-21 \le h \le 11$ $-6 \le k \le 10$ $-6 \le l \le 10$	$-6 \le h \le 6$ $-10 \le k \le 10$ $-19 \le l \le 20$
Extinction coefficient, k[a]	0.0067 (7)	–
Refined parameters	90	192
R-indices [$I > 2\ \sigma(I)$][b]	$R_1=0.020$ $wR_2=0.051$	$R_1=0.036$ $wR_2=0.083$
R-indices (all data)[b]	$R_1=0.026$ $wR_2=0.052$	$R_1=0.043$ $wR_2=0.086$
Goodness-of-fit, S	0.98	1.16
$(\Delta/\sigma)_{max}$	0.001	0.001
$(\Delta\rho)_{max}$, $(\Delta\rho)_{min}$ (e Å^{-3})	0.30–0.26	1.49–0.77

[a] $F_c^*=F_c k[1+0.001F_c^2\lambda^3/\sin(2\theta)]^{-1/4}$.
[b] $w=1/[\sigma^2(F_o^2)+(0.0310P)^2+0.0000P]$ for **1**, and $w=1/[\sigma^2(F_o^2)+(0.0300P)^2+4.7382P]$ for **2**, where $P=(F_o^2+2F_c^2)/3$.

Table 2
Selected bond distances (Å) and bond angles (°) in **1** and **2**.

1

Zn1–O3	1.9167 (12)	N1–C1	1.470 (2)	O3–P1–O2	109.92 (7)
Zn1–O3^{i}	1.9167 (12)	N2–C2	1.475 (2)	O3–P1–O1	107.37 (7)
Zn1–O4^{ii}	1.9545 (12)	C1–C2	1.511 (3)	O2–P1–O1	109.75 (9)
Zn1–O4^{iii}	1.9545 (12)	O3–Zn1–O3^{i}	115.27 (7)	O3–P1–O4	111.33 (8)
⟨Zn1–O⟩ [a]	1.936 (11)	O3–Zn1–O4^{ii}	113.20 (5)	O2–P1–O4	107.93 (8)
P1–O3	1.5281 (12)	O3^{i}–Zn1–O4^{ii}	101.12 (5)	O1–P1–O4	110.55 (7)
P1–O2	1.5327 (12)	O3–Zn1–O4^{iii}	101.12 (5)	P1–O3–Zn1	145.25 (9)
P1–O1	1.5339 (14)	O3^{i}–Zn1–O4^{iii}	113.20 (5)	**P1–O4–Zn1^{iv}**	**129.40 (8)**
P1–O4	1.5411 (13)	O4^{ii}–Zn1–O4^{iii}	113.51 (8)		
⟨P1–O⟩ [a]	1.534 (3)				

Symmetry codes: (i) $-x+3/2$, $-y+1/2$, z; (ii) x, $-y+1/2$, $z-1/2$; (iii) $-x+3/2$, y, $z-1/2$; (iv) $-x+3/2$, y, $z+1/2$.

2

Zn1–O13^{i}	1.912 (4)	P2–O23	1.524 (4)	O34–Zn3–O31^{v}	103.18 (17)
Zn1–O12^{ii}	1.928 (4)	P2–O22	1.526 (4)	O32^{vi}–Zn4–O22	103.66 (18)
Zn1–O21	1.985 (4)	P2–O21	1.569 (4)	O32^{vi}–Zn4–N1	121.3 (2)
Zn1–O11	2.009 (4)	⟨P2–O⟩ [a]	1.536 (11)	O22–Zn4–N1	110.2 (2)
⟨Zn1–O⟩ [a]	1.959 (23)	P3–O34	1.521 (4)	O32^{vi}–Zn4–O31^{v}	111.15 (17)
Zn2–O14^{iii}	1.903 (4)	P3–O33	1.521 (4)	O22–Zn4–O31^{v}	105.39 (17)
Zn2–O24	1.933 (4)	P3–O32	1.529 (4)	N1–Zn4–O31^{v}	104.3 (2)
Zn2–O21^{iv}	1.970 (4)	P3–O31	1.564 (4)	O14–P1–O13	110.7 (2)
Zn2–O11	2.001 (4)	⟨P3–O⟩ [a]	1.534 (10)	O14–P1–O12	107.3 (2)
⟨Zn2–O⟩ [a]	1.952 (21)	O13^{i}–Zn1–O12^{ii}	120.42 (18)	O13–P1–O12	112.0 (2)
Zn3–O33^{iv}	1.921 (4)	O13^{i}–Zn1–O21	103.76 (16)	O14–P1–O11	110.6 (2)
Zn3–O23	1.936 (4)	O12^{ii}–Zn1–O21	103.42 (17)	O13–P1–O11	110.6 (2)
Zn3–O34	1.944 (4)	O13^{i}–Zn1–O11	114.77 (17)	O12–P1–O11	105.4 (2)
Zn3–O31^{v}	1.984 (4)	O12^{ii}–Zn1–O11	106.96 (17)	O24–P2–O23	109.5 (2)
⟨Zn3–O⟩ [a]	1.946 (13)	O21–Zn1–O11	105.89 (15)	O24–P2–O22	111.3 (3)
Zn4–O32^{vi}	1.916 (4)	O14^{iii}–Zn2–O24	115.99 (18)	O23–P2–O22	112.6 (2)
Zn4–O22	1.931 (4)	O14^{iii}–Zn2–O21^{iv}	112.57 (17)	O24–P2–O21	108.0 (2)
Zn4–N1	1.961 (5)	O24–Zn2–O21^{iv}	109.31 (16)	O23–P2–O21	108.4 (2)
Zn4–O31^{v}	1.994 (4)	O14^{iii}–Zn2–O11	112.18 (17)	O22–P2–O21	106.8 (2)
⟨Zn4–O⟩ [a]	1.947 (17)	O24–Zn2–O11	99.77 (16)	O34–P3–O33	111.6 (2)
P1–O14	1.520 (4)	O21^{iv}–Zn2–O11	105.90 (16)	O34–P3–O32	110.5 (2)
P1–O13	1.521 (4)	O33^{iv}–Zn3–O23	112.34 (18)	O33–P3–O32	110.1 (2)
P1–O12	1.534 (4)	O33^{iv}–Zn3–O34	115.67 (16)	O34–P3–O31	108.9 (2)
P1–O11	1.570 (4)	O23–Zn3–O34	104.63 (17)	O33–P3–O31	108.3 (2)
⟨P1–O⟩ [a]	1.536 (12)	O33^{iv}–Zn3–O31^{v}	113.16 (16)	O32–P3–O31	107.4 (2)
P2–O24	1.523 (4)	O23–Zn3–O31^{v}	106.95 (17)		

Symmetry codes: (i) $x+1$, y, z; (ii) $-x+1$, $-y+1$, $-z+2$; (iii) $-x+1$, $-y+2$, $-z+2$; (iv) $x-1$, y, z; (v) $-x+2$, $-y+1$, $-z+1$; (vi) x, $y+1$, z; (vii) x, $y-1$, z.

[a] Calculated as $\sigma_d = \sqrt{\Sigma_m (d_m - \overline{d})^2 / m(m-1)}$.

Table 3
Hydrogen bond geometry (Å,°) in **1** and **2**. For comparison, less probable hydrogen bonds are given in italics.

D–H···*A*	D–H	H···A	< D–H · · · A	D···A
1				
N1–H11···O1^{v}	0.89	2.129	142.76	2.888(2)
N1–H11···O2^{v}	*0.89*	*2.386*	*149.80*	*3.187(2)*
N1–H12···O1	0.89	1.974	171.45	2.858(2)
N1–H12···O3	*0.89*	*2.474*	*112.46*	*2.932(2)*
N1–H13···O1^{ii}	0.89	1.844	168.57	2.722(2)
N2–H21···O2^{ix}	0.89	1.883	159.79	2.736(2)
N2–H22···O4^{i}	0.89	1.939	165.63	2.810(2)
N2–H23···O2^{vi}	0.89	1.913	161.54	2.772(2)

Symmetry codes: (i) $-x+3/2$, $-y+1/2$, z; (ii) x, $-y+1/2$, $z-1/2$; (v) $-x+2$, $y-1/2$, $-z+1/2$; (vi) x, $-y+1/2$, $z+1/2$; (ix) x, $y-1$, z.

2

N1–H11···O33^{viii}	0.89	2.383	159.68	3.232(8)
N1–H12···O24^{i}	0.89	2.448	167.19	3.322(8)
N1–H12···O22^{i}	*0.89*	*2.553*	*131.28*	*3.210(8)*
N1–H13···O32^{ix}	0.89	2.224	139.78	2.960(6)
N1–H13···O33^{vi}	*0.89*	*2.54*	*131.72*	*3.201(7)*
N2–H21···O13^{x}	0.89	2.271	137.34	2.987(7)
N2–H22···O34^{iv}	0.89	2.382	157.62	3.221(7)
N2–H22···O23^{iv}	*0.89*	*2.55*	*121.77*	*3.114(8)*
N2–H23···O12^{ii}	0.89	2.087	148.48	2.880(7)
N2–H23···O14^{ii}	*0.89*	*2.757*	*113.21*	*3.212(9)*
N2–H24···O22^{xi}	0.89	2.443	172.19	3.325(8)

Symmetry codes: (i) $x+1$, y, z; (ii) $-x+1$, $-y+1$, $-z+2$; (iv) $x-1$, y, z; (vi) x, $y+1$, z; (viii) $-x+3$, $-y+1$, $-z+1$; (ix) $x+1$, $y+1$, z; (x) $-x$, $-y+1$, $-z+2$; (xi) $x-1$, $y-1$, z.

Si-based, Peltier-cooled charge-coupled device (CCD) detector, and a software-controlled *x*–*y* stage. The spectral dispersion was done using a diffraction grating with 1800 grooves/mm. Spectra were excited with the He–Ne 632.8 nm and Ar 472.97 nm emissions for **1** and **2**, respectively. Olympus 50× and 100× objectives with NA=0.90 were used for **1** and **2**, respectively, and the system was operated in confocal mode.

3. Results and discussion

3.1. Crystal structure of $(H_3NCH_2CH_2NH_3)_2[Zn(\mu\text{-}PO_4)_2]$ (**1**)

The crystal structure of **1** consists of infinite inorganic $ZnP_2O_8^{4-}$ chains running along the [0 0 1] direction. They are interconnected by hydrogen bonds formed between NH_3 groups from diprotonated ethylenediammonium cations, H_2en^{2+} and O atoms from adjacent chains (Fig. 1a). In **1** the zinc atom situated at special position 4*d* is coordinated by two symmetry equivalents of O3 and O4 with an average Zn1–O distance of 1.94(1) Å, providing a slightly distorted tetrahedral geometry (Table 2, Fig. 1). This distance is very close to the value (1.95 Å) calculated from the sum of effective ionic radii for the Zn^{2+} and O^{2-} ions (0.60 and 1.35 Å for four-coordinated Zn^{2+} and two-coordinated O^{2-}, respectively [15]). All four O atoms of the ZnO_4 tetrahedra are double coordinated and, consequently, Zn atoms are connected to the four neighboring P atoms via Zn–O–P bridges. In that way each ZnO_4 is joined to four PO_4, while each PO_4 is attached to two ZnO_4 tetrahedra having one common O atom (Fig. 1). The phosphorus atom is positioned in the general position and exhibits nearly regular tetrahedral coordination with P–O distances ranging between 1.5281(12) and 1.5411(13) Å and an average P–O distance of 1.534(3) Å, which is in agreement with the calculated value (1.52 Å) for the sum of effective ionic radii for the P^{5+} and O^{2-} ions [15]. Two ZnO_4 and two PO_4 tetrahedra are connected through their oxygen vertices form 4M rings of tetrahedral centers. The 4M rings are further linked via O–Zn–O bridges (Fig. 1).

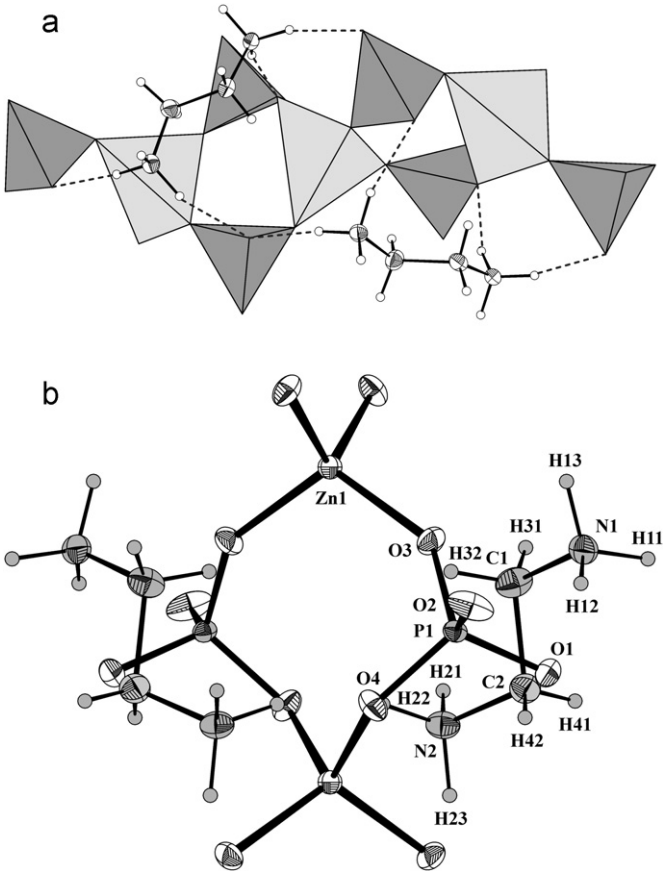

Fig. 1. (a) Polyhedral representation of the structure of **1** showing $ZnP_2O_8^{4-}$ chains of ZnO_4 (larger, light shading) and PO_4 (smaller, dark shading) vertex-sharing tetrahedra with two H_2en^{2+} cations. Ellipsoids represent C and N atoms. (b) Structure of **1** in the *ac* plane showing ZnO_4 and PO_4 tetrahedra in inorganic $ZnP_2O_8^{4-}$ chain extending along [0 0 1] (*a*-axis is horizontal) and H_2en^{2+} cations with atom labeling scheme. (Displacement ellipsoids are drawn at the 50% probability level, spheres for H atoms are of arbitrary radii.)

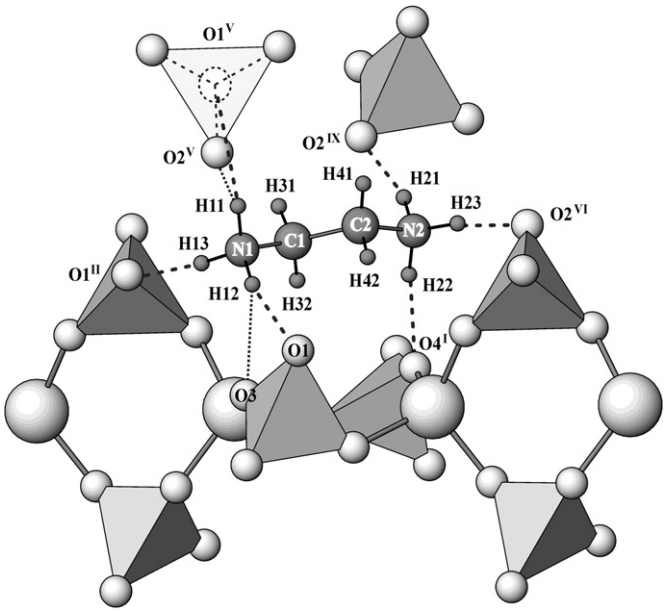

Fig. 2. Structural fragment of **1** showing a network of hydrogen bonds (bold dashed lines) between NH_3 groups from H_2en^{2+} cations and oxygen atoms from inorganic $ZnP2O_8^{4-}$ chains. Dotted lines represent less probable hydrogen bonds. [Symmetry codes: (i) $-x+3/2, -y+1/2, z$; (ii) $x, -y+1/2, z-1/2$; (v) $-x+2, y-1/2, -z+1/2$; (vi) $x, -y+1/2, z+1/2$; (ix) $x, y-1, z$.]

The interchain space is filled by H_2en^{2+} cations that interconnect the chains through a network of hydrogen bonds. The H_2en^{2+} adopts *anti* conformation with a dihedral angle N1–C1–C2–N2 of 168.1(2)°. Two N atoms (from $N1H_3$ and $N2H_3$) act as triple hydrogen bond donors. Both NH_3 groups are individually linked to oxygens from different inorganic chains (Fig. 2).

The first $N1H_3$ group is hydrogen bonded to three symmetrically equivalent O1 atoms, while the second $N2H_3$ group is hydrogen bonded to two O2 and one O4 atoms (Fig. 2), with N···O distances between 2.722(2) and 2.888(2) Å (Table 3). These distances indicate the presence of moderately strong hydrogen bonds. Around N1 there are two further oxygen atoms at longer distances 2.932(2) (O3) and 3.187(2) Å ($O2^{v}$), symmetry code: (v) $-x+2, y-1/2, -z+1/2$), demonstrating that additional orientations are also possible due to disorder of the $N1H_3$ group. In the structure refinement it was assumed that both NH_3 groups were completely in one orientation.

The bond-valence calculations [16,17] show that the Zn–O and P–O bond lengths are consistent with the presence of divalent zinc and pentavalent phosphorus. The bond-valence sums for the terminated O1 and O2, which are attached to phosphorus only, are significantly undersaturated (Σv_{ij} is 1.25 and 1.26 v.u. for O1 and O2, respectively) indicating that both oxygens act as triple hydrogen bond acceptors. This is obvious for O1. Assuming the rotation of $N1H_3$ groups, O2 can also serve as a triple hydrogen bond acceptor. The bond-valence sums for the bicoordinate oxygens O3 and O4 are slightly undersaturated (Σv_{ij} is 1.83 and 1.74 v.u. for O3 and O4, respectively) showing that O3 and O4 are

single hydrogen bond acceptors. Again, this is obvious for O4, while for O3 it is possible in the case of differently oriented $N1H_3$ groups.

3.2. Crystal structure of $(NH_4)[(H_3N)Zn\{(\mu\text{-}PO_4)Zn\}_3]$ (2)

The characteristic feature of **2** is the occurrence of both, Zn–O–P and Zn–O–Zn linkages. The Zn:P ratio in **1** is 1:2, and there are no Zn–O–Zn bridges. A higher Zn content in **2** (Zn:P ratio of 4:3) implies some Zn–O–Zn linkages, with bridging oxygen atoms in trigonal coordination and an additional link to a phosphorus atom. Consequently, besides 4M rings, the 3M rings of tetrahedral centers were formed. Therefore, considering the network of Zn–O and P–O bonds, the crystal structure of **2** can be described as composed of 3M and 4M tetrahedral rings generated from the vertex linking of PO_4 and $Zn\varphi_4$ (φ is O or NH_3) tetrahedra (Fig. 3a). In addition to Zn–O–Zn bonding and 3M ring units, the structure of **2** displays another typical feature of ZPOs, i.e. the 3D framework of **2** contains 8M-ring channels running along [1 0 0] (Fig. 3b).

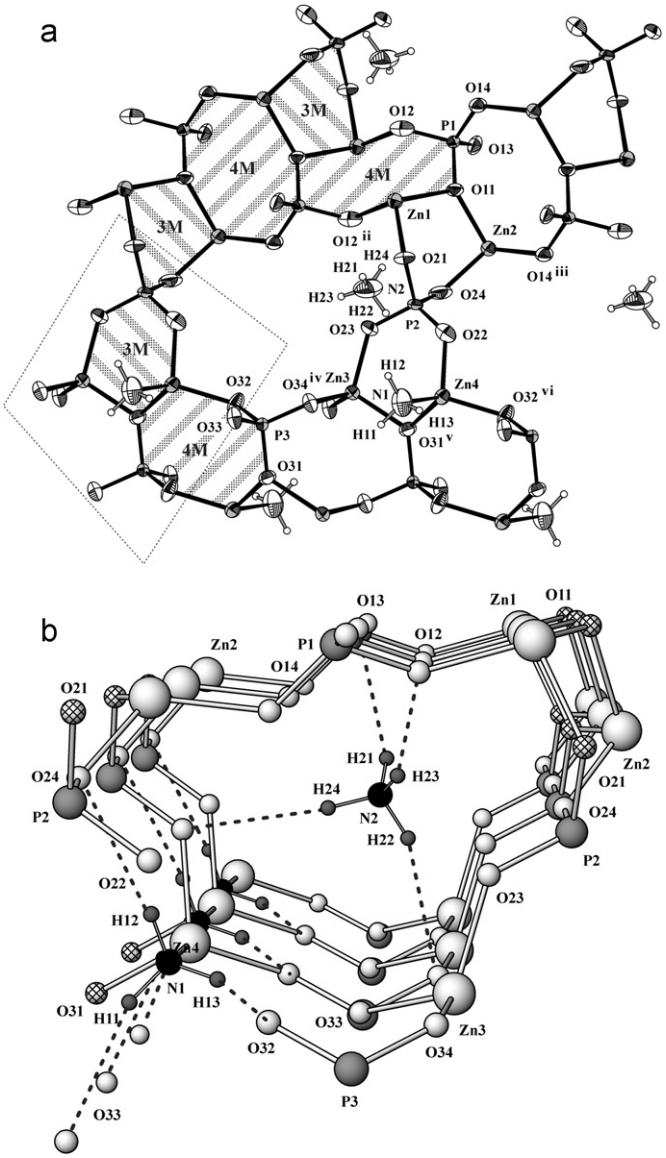

Fig. 3. (a) Details of the structure of **2** viewed approximately along [1 1 0] (*c*-axis is vertical) showing the 3M-ring/4M-ring tetrahedral connectivity with atomic numbering scheme. Structural unit formed by sharing vertices among $Zn3O_4$, $Zn4O_3(NH_3)$, $P3O_4$ and $P2O_4$ is framed. [Displacement ellipsoids are drawn at the 80% probability level; symmetry codes: (i) $x+1, y, z$; (ii) $-x+1, -y+1, -z+2$; (iii) $-x+1, -y+2, -z+2$; (iv) $x-1, y, z$; (v) $-x+2, -y+1, -z+1$; (vi) $x, y+1, z$.] (b) Perspective view of 8M channels and NH_4^+ cations in the structure of **2** oriented approximately along [1 0 0] (*b*-axis is horizontal). Hachured O atoms are three-coordinated and not involved in hydrogen bonding.

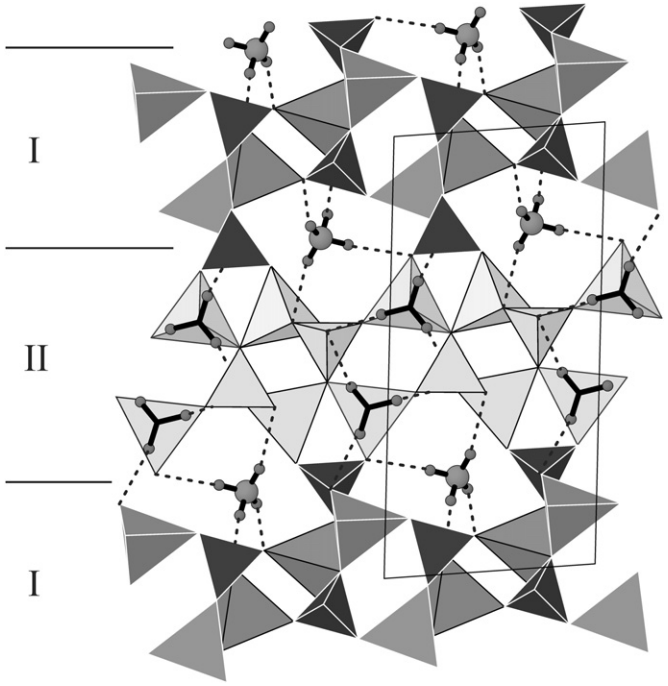

Fig. 4. Projection of the structure of **2** along [1 0 0] (*c*-axis is vertical) showing ZnO_4, PO_4 and $ZnO_3(NH_3)$ tetrahedra in layers I (larger, grey shading for ZnO_4 and smaller, black shading for PO_4) and II [larger, for ZnO_4 and $ZnO_3(NH_3)$ and smaller for PO_4, light grey shading for all]. In the channels NH_4^+ ions are situated. (Spheres for N_2 and H are of arbitrary radii. Dashed lines represent hydrogen bond interactions.)

The framework of formula $[(H_3N)Zn\{(\mu\text{-}PO_4)Zn\}_3]^-$ is charge balanced by ammonium cations located inside the 8M channels of tetrahedral Zn2–P1–Zn1–P2–Zn3–P3–Zn4–P2 centers. The rings are linked in the *a*-direction by only two Zn–O–P bridges (Zn2–O21–P2 and Zn3–O33–P3) forming the walls of the channel (Fig. 3b). Using the program PLATON [18] the volume of the void was calculated as 47.5 Å^3, which is 7.6% of the unit cell volume (624.5 Å^3). The calculated center of the void (0.851 0.684 0.230) is very close to the coordinates found for N2 (0.837 0.663 0.219).

The 3D open framework structure of **2** has a pseudo-layered character and can be divided into two types of regularly alternating corrugated layers, which share common $P2O_4$ tetrahedra and are parallel to (0 0 1) plane (Fig. 4). The bordering $P2O_4$ tetrahedra join the layers together; they are placed in such a way that two oxygens (O24 and O21) are linked to the layer I, and another two (O22 and O23) to the layer II. Hydrogen bond interactions contribute additionally to the connectivity. Excluding $P2O_4$ tetrahedra, both types of layers contain two crystallographically distinct Zn sites and one P site. The layer I is positioned between $z \approx -0.33$ and 0.33, and hosts $Zn1O_4$, $Zn2O_4$ and $P1O_4$ coordination tetrahedra. The layer II is situated in the central part of unit cell and is composed from $Zn3O_4$, $Zn4O_3(NH_3)$ and $P3O_4$ coordination tetrahedra. Its boundaries lie between $z \approx 0.33$ and 0.67.

The main difference between layers is the presence of coordinated NH_3 molecules in layer II and infinite Zn1–O11–Zn2–O21–Zn1 chains in layer I (Fig. 4). There are no such chains in layer II, where groups of two Zn-tetrahedra, $Zn3O_4$ and $Zn4O_3(NH_3)$ share only one oxygen, O31, in trigonal coordination. With exception of

terminal NH_3 group, these tetrahedra share all vertices with adjacent PO_4 tetrahedra.

The structure of **2** can be alternatively described as consisting of three similar basic structural units, which are formed by sharing vertices among two ZnO_4 and two PO_4 tetrahedra: $Zn1O_4$, $Zn2O_4$, $P1O_4$ with $P2O_4$ are involved in building two, while $Zn3O_4$, $Zn4O_3(NH_3)$, $P3O_4$ and again with $P2O_4$ in forming one such structural unit. As an example, one structural unit is framed in Fig. 3a. Similar basic structural units have been observed not only in the structures with Zn:P ratio of 4:3, but also in compounds with Zn:P ratio of 1:1, like $(NH_4)[Zn_2(PO_4)(PO_3(OH))]$ [19], $(NH_4)[Zn_{2-x}Co_x(PO_4)(PO_3(OH))]$ ($x\sim0.12$) [20], as well as in $NaH(ZnPO_4)_2$ and $CsH(ZnPO_4)_2$ [21].

Isolated from each other, all PO_4 tetrahedra are rather regular with a small angular variation of the O–P–O angles ranging between 105.4(2) and 112.6(2)°, while O–Zn–O angles deviate more and range from 99.8(2) to 121.3(2)° (Table 2). The bond distances for the tricoordinate oxygens (O11, O21 and O31) are longer and are in the intervals of 1.564(4)–1.570(4) and 1.984(4)–2.009(4) Å for P–O and Zn–O, respectively. The average Zn4–O distance is slightly shorter [1.95(2) Å] than Zn4–N bond length (1.961(5) Å).

The results of bond-valence calculations confirm the presence of divalent zinc and pentavalent phosphorus. The bond-valence sum for the tricoordinate oxygens O11, O21 and O31 are slightly oversaturated (Σv_{ij} is 2.03, 2.10 and 2.08 v.u. for O11, O21 and O31, respectively), while the bicoordinate oxygen atoms are somewhat undersaturated (Σv_{ij} is 1.80, 1.87, 1.88, 1.82, 1.82, 1.83, 1.83 1.86 and 1.82 v.u. for O12, O13, O14, O22, O23, O24, O32, O33 and O34, respectively). Taking into account that O12, O13, O22, O24, O32, O33 and O34, as well as O14 and O23 (see explanation below), are single hydrogen bond acceptors from $N1H_3$ and $N2H_4$ groups, the bond valences are well balanced.

The coordinated ammonia molecules $N1H_3$ are connected to framework O33, O24, and O32 atoms by relatively weak hydrogen bonds with N···O distances between 2.960(6) and 3.322(8) Å. In the structure refinement, it was assumed that the ammonium molecule is completely in one orientation, although there were indications suggesting that additional orientations are present (Table 3). However, a comprehensive constrained refinement produced reliable geometry. The ammonium ion $N2H_4^+$ is hydrogen bonded to four framework O atoms with N···O distances ranging from 2.880(7) to 3.325(8) Å. According to the refined structural model, all bicoordinate oxygens, except O14 and O23, act as single hydrogen bond acceptors. Assuming rotation of $N2H_4^+$ group and according to N2···O distances (Table 3) and bond valence calculations, O14 and O23 can also serve as hydrogen bond acceptors in the case of differently oriented $N2H_4^+$ groups.

3.3. *Raman spectra of **1** and **2***

The Raman spectra of **1** and **2** are shown in Fig. 5a and b. The precise assignment of all the features present in the spectra is pretty complicated by the large number of observed bands and by the fact that many vibrations due to the different group of atoms fall in the same spectral range. However, the distinct frequency ranges may be assigned as follows.

The high frequency spectral region of **1** (from 4000 to 1200 cm^{-1}) of small intensity shows the NH_2 and CH_2 stretching and bending modes (Fig. 5a). The peaks at 3015 (vw), 2996 (m) and 2979(m) belong to N–H asymmetric and symmetric stretches [22], the frequencies of which have been lowered due to the hydrogen bonding [23]. The peaks at 2954 (w) and 2930 (w) cm^{-1} belongs to C–H asymmetric stretches and bands at 2914 (w), 2893 (vw) and 2810 (w) cm^{-1} to C–H symmetric stretches [24,25].

Very weak and broad Raman bands between ~2700 and 2000 cm^{-1} are probably due to ν(N–H···O) [24]. The shift of the bands to this region indicate involvement of the amine groups in hydrogen bonds of various strength [26], which is in well agreement with the structural study ((N)–H···O–(P)=1.913–2.129 Å, see also Table 3) and correlation of stretching frequencies as a function of distances in hydrogen bonds given by Ref. [23]. The asymmetric and symmetric NH_2 deformation are observed as weak bands at 1664, 1617 and 1584 cm^{-1} in the spectrum. The CH_2 deformation are represented with bands at 1502 (vw), 1486 (w), 1456 (m) and 1413 (w) cm^{-1}. The CH_2 twisting and wagging modes are represented by bands at 1372 (vw), 1356 (vw) cm^{-1}, 1330(m), 1280(m) and 1264 (vw) cm^{-1} [24,22].

Bands below 1200 cm^{-1} are due to vibrations of the PO_4 and ZnO_4 groups and due to lattice modes. The peaks between 1200 and 750 cm^{-1} present asymmetric and symmetric P–O stretches. In the region below 750 cm^{-1} the bending modes of the PO_4 groups, vibrations of ZnO_4 and various lattice modes of the compound appear.

The Raman spectrum of **2** reflects the complexity of the crystal structure and shows a strong similarity to structurally related

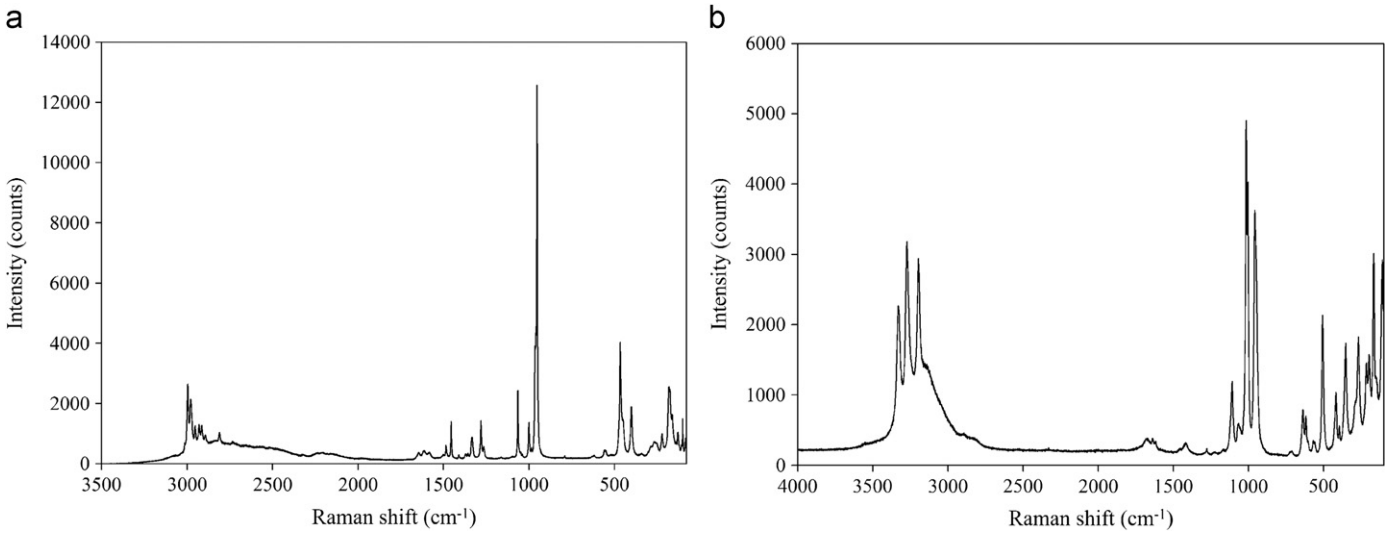

Fig. 5. Single-crystal Raman spectra of compounds **1** (a) and **2** (b).

ammonium-(zinc, gallium)-phosphates with framework topologies of analcime and paracelsian type [27,28]. The considerably large number of bands is caused by the three crystallographically different PO_4 tetrahedra and four crystallographically different $Zn\varphi_4$ (φ is O or NH_3) tetrahedra, as well as NH_3 molecule and NH_4^+ group. Previously published spectral data on orthophosphates containing both NH_4^+ group and coordinated NH_3 molecule are rather poor. Therefore, attempts to compare with them failed. Nevertheless, the distinct frequency ranges may be assigned as follows.

The high frequency spectral region (4000–1200 cm^{-1}) of medium intensity shows the N–H stretching and bending modes (Fig. 5b). The stretching vibrations of N–H and N–H···O can be observed between 3400 and 2700 cm^{-1} [25]. The weak bands between 1700 and 1250 cm^{-1} can be attributed to the bending modes of NH_3 molecule and NH_4^+ cation [25].

Bands below 1200 cm^{-1} are due to vibrations of the PO_4 and $Zn\varphi_4$ groups and due to lattice modes. The peaks between 1200 and 750 cm^{-1} present asymmetric and symmetric P–O stretches. In the region below 750 cm^{-1} the bending modes of the PO_4 groups and various lattice modes of the compound appear.

3.4. Relationships to similar structures

In order to systematize the structural characteristics of similar open framework ZnPOs and AlPOs, it is worthwhile to compare **1** and **2** with compounds containing $MP_2O_8^{4-}$ (M=Zn, Al) chains, as in **1**, or open framework structures of corner-shared tetrahedra with Zn:P ratio of 4:3, as in **2**.

A survey of crystallographic databases gave in total 8 compounds with M:P ratio of 1:2 including MO_4 and PO_4, $PO_3(OH)$ or $PO_2(OH)_2$ tetrahedra, which are linked to form infinite chains of vertices-sharing polyhedra. In addition, there are two related compounds: $Cd_2[Cu(PO_4)_2]\cdot H_2O$, where Cu is in a square-pyramidal coordination [29], and $[Zn(H_2O)_2(PO_2(OH)_2)_2]\cdot 2paba$ ($paba$=$H_2NC_6H_4COOH$) [4], with Zn in an octahedral coordination. The chemical formulae, abbreviations, references and some additional data are given in Table 4, while the selected basic chain units are shown in Fig. 6. The compounds are mainly prepared by hydro- or ionothermal synthesis. All structures are of low, triclinic to orthorhombic symmetry with predominance of space group $P2_1/c$. In some cases (e.g. [5,30,31]), short P–O distances of about 1.5 Å, indicating double P=O bonds character, were observed.

The chain structures can accommodate some degree of flexibility, which can be expressed by the "chain twist angle", i.e. the angle between planes of neighboring 4M rings defined by two M and two P atoms. As seen in Table 4, this angle could vary between 0° and 85°. However, in the last two cases the angle is constrained to 0° due to requirements of exceptional (square-planar or octahedral) geometry. Therefore, the actual range is much narrower, from about 58° to 85°.

There are remarkable similarities between **1** and the structures of $(NH_4)(1,2\text{-}H_2dap)[Al(PO_4)_2]$ [30] and $(NH_4)(H_2en)[Al(PO_4)_2]$ [5], although both aluminophosphates contain additional NH_4^+ cations to keep charge balance. These three compounds, together with $(C_7H_{10}N)[Al(PO_3(OH))_2]$ [31], make a group with high chain twist angles (mean value 83°). The mean value for remaining five structures is 68° and they always contain protonated phosphate groups. Consequently, it seems that the presence of intra- and interchain hydrogen bonds involving HPO_4^{2-} groups is the main factor determining the value of chain twist angle, with the angle decreasing with increasing number of such hydrogen bonds. This is supported by the lowest angle in $(NH_4)[Zn(PO_3(OH))(PO_2(OH)_2)]$ [33], where $H_2PO_4^-$ groups are present too.

Table 4
Chain twist angles for the chain phosphates with M:P ratio of 1:2 (M=Zn, Al, Cu).

No.	Formula	Symmetry, space group	Chain twist angle (°)	Reference
1	$(H_2en)[Zn(\mu\text{-}PO_4)_2]$, $H_2en=C_2H_{10}N_2^{2+}$=diprotonated ethylenediamine	Orthorhombic, *Pccn*	85.0	This work
2	$(NH_4)(1,2\text{-}H_2dap)[Al(PO_4)_2]$, $H_2dap=C_3H_{16}N_3^{2+}$ diprotonated 1,2-diaminopropane	Orthorhombic, $Pc2_1n$	84.6	[30]
3	$(NH_4)(H_2en)[Al(PO_4)_2]$	Orthorhombic, *Pccn*	82.2	[5]
4	$(C_7H_{10}N)[Al(PO_3(OH))_2]$, $C_7H_{10}N^+$=protonated 1-ethylpyridine	Monoclinic, $P2_1/c$	78.7	[31]
5	$(C_{10}H_{22}N_4)[Zn(PO_3(OH))_2]\cdot 2H_2O$, $C_{10}H_{22}N_4$=bis-(aminopropyl)piperazine	Orthorhombic, *Pbca*	71.9	[32]
6	$(C_6H_{11}N_2)[Al(PO_3(OH))_2]$, $C_6H_{11}N_2^+$=protonated 1-ethyl-3-methylimidazoline, modification I	Monoclinic, $P2_1/c$	71.1	[31]
7	$(C_6H_{11}N_2)[Al(PO_3(OH))_2]$, $C_6H_{11}N_2^+$=protonated 1-ethyl-3-methylimidazoline, modification II	Triclinic, $P\bar{1}$	70.3	[31]
8	$(C_5H_{14}N_2)[Zn(PO_3(OH))_2]$, $C_5H_{14}N_2^+$=protonated methylpiperazine	Monoclinic, $P2_1/c$	66.4	[32]
9	$(NH_4)[Zn(PO_3(OH))(PO_2(OH)_2)]$	Triclinic, $P\bar{1}$	58.4	[33]
10	$[Zn(H_2O)_2(PO_2(OH)_2)_2]\cdot 2paba$, paba=$C_7H_7N$=p-aminobenzoic acid	Monoclinic, $P2_1/c$	0	[4]
11	$Cd_2[Cu(PO_4)_2]\cdot H_2O$	Triclinic, $P\bar{1}$	0	[29]

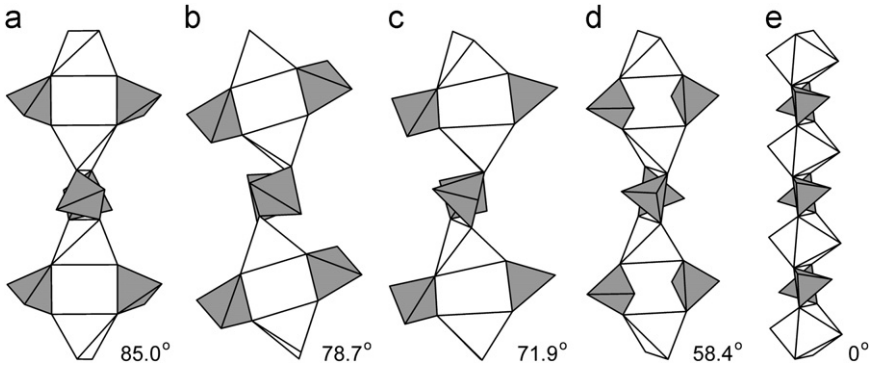

Fig. 6. Characteristic examples and the corresponding chain twist angles of basic units in chain phosphates with M:P (M=Zn, Al) ratio of 1:2. (a) **1**, (b) $(C_7H_{10}N)[Al(PO_3(OH))_2]$, (c) $(C_{10}H_{22}N_4)[Zn(PO_3(OH))_2]\cdot 2H_2O$, (d) $(NH_4)[Zn(PO_3(OH))(PO_2(OH)_2)]$, (e) $[Zn(H_2O)_2(PO_2(OH)_2)_2]\cdot 2paba$. (For abbreviations and references, see Table 4.)

Table 5
Framework dimensionality and tetrahedral atom density for the ZPOs with Zn:P ratio of 4:3.

No.	Formula	Symmetry, space group	T-atom density	Reference
	2D			
1	(Htea)[$Zn_4(pbc)_3$], Htea=$C_6H_{16}N^+$=protonated triethylamine, pbc^{3-}=$OOCC_6H_4PO_3$, anion of 4-phosphono-benzoic acid, H_3pbc	Monoclinic, $P2_1$	7.55	[35]
2	$(Hdabco)_2[Zn_8(pbc)_6]\cdot 6H_2O$, Hdabco=$C_6H_{12}N_2^+$=protonated 1.4-diazabicyclo[2.2.2]octane	Trigonal, $R\bar{3}$	8.61	[44]
3	$(C_3H_4N_2)_3[Zn_{(4-x)}Co_x(PO_3(OH)(PO_4)_2)]$ (x=0.25), $C_3H_4N_2$=imidazole	Triclinic, $P\bar{1}$	13.29	[47]
4	$(C_3H_4N_2)_3[Zn_4(PO_3(OH))(PO_4)_2]$	Triclinic, $P\bar{1}$	13.39	[45,46]
	3D			
5	$Rb_{2.906}[Zn_4O(PO_4)_3]\cdot 3.524H_2O$	Cubic,$F\bar{4}3c$	15.51	[41][a]
6	$(CH_6N)_3[Zn_4O(PO_4)_3]$, CH_6N^+=protonated methylamine	Monoclinic, $P2_1$	15.68	[36]
7	$Na_3[Zn_4O(PO_4)_3]\cdot 6H_2O$	Trigonal, $R3c$	15.90	[41][a]
8	$(C_6H_{17}N_3)[Zn_4(OH)(PO_4)_3]$, $C_6H_{17}N_3^{2+}$=diprotonated 1-(2-aminoethyl)piperazine	Triclinic, $P\bar{1}$	17.68	[40]
9	$(C_3H_{10}N)[Zn_4(H_2O)(PO_4)_3]$, $C_3H_{10}N^+$=protonated trimethylamine	Triclinic, $P\bar{1}$	18.76	[34]
10	$(C_3H_6N_2)[Zn_4(OH)(PO_4)_3]$, $C_3H_6N_2^{2+}$=diprotonated imidazole	Monoclinic, $P2_1/n$	19.28	[49]
11	$(C_2H_8N)(H_3O)[Zn_4(H_2O)(PO_4)_3]_2\cdot H_2O$, $C_2H_8N^+$=protonated dimethylamine	Orthorhombic, $Pnn2$	19.92	[39,37]
12	$(C_2H_8N)[Zn_4(H_2O)(PO_4)_3]$, $C_2H_8N^+$=protonated ethylamine	Monoclinic, $P2_1/n$ (14)	19.97	[50,48]
13	$(NH_4)[(H_3N)Zn\{(\mu\text{-}PO_4)Zn\}_3]$	Triclinic, $P\bar{1}$	22.42	This work
14	$(CH_6N)[Zn_4(PO_4)_3]$, CH_6N^+=protonated methylamine	Orthorhombic, $Pbca$	22.71	[51]
15	$H[Zn_4(PO_4)_3]\cdot H_2O$	Triclinic, $P\bar{1}$	23.70	[34]
16	$(NH_4)(H_3O)[Zn_4(PO_4)_3]_2\cdot H_2O$	Triclinic, $P\bar{1}$	23.90	[38]
17	$K[Zn_4(PO_4)_3]$	Orthorhombic, $Pccn$	25.66	[48]

[a] Only two members of the series of isostructural compounds with the general formula $M_3[Zn_4O(XO_4)_3](H_2O)_n$ (M=Na, K, Rb, Cs; X=P, As; n=3–6) [41,42], are listed in Table 5, as an example.

According to Bu and coworkers [34] in open framework ZPOs the Zn:P ratio not frequently exceeds one. However, in the structure of **2** a higher Zn:P ratio of 4:3 was found, and to the best of our knowledge, the same ratio exists in at least 16 other ZPOs (Table 5). The feature common to such ZPOs is that they are composed of tetrahedrally coordinated Zn and P atoms. Adjacent corner-sharing tetrahedra form layers (2D structures) or an open framework (3D structures), both with 1D channels. The first four compounds listed in Table 5 have 2D (layered) structures, and all other have 3D open framework structures with inorganic ions or organic molecules and ions as guest species.

The "openness" of a structure can be described in terms of the tetrahedral (T) atom density defined as the number of T-atoms per 1000 Å^3 [37]. The values of T-atom densities for known structures with Zn:P ratio equal to 4:3 are also listed in Table 5. The T-atom density for **2** is 22.42. This value, a small channels volume (only 7.6% of the unit cell) and the presence of 25% trigonally coordinated oxygen atoms indicate that **2** belongs to the more condensed structure rather than to the open ones.

In the 3D open framework structures listed in Table 5, different channels are present. They all have 8M-ring channels, with additional 6M channels in three of them: $H[Zn_4(PO_4)_3]\cdot H_2O$ [34], $(NH_4)(H_3O)[Zn_4(PO_4)_3]_2\cdot H_2O$ [38] and $(C_2H_8N)(H_3O)[Zn_4(H_2O)(PO_4)_3]_2\cdot H_2O$ [39]. Specially, in the 3D structure of $(C_6H_{17}N_3)[Zn_4(OH)(PO_4)_3]$ [40] exist 12M- and 8M-ring channel systems, in which $C_6H_{17}N_3$ and a terminal OH group that coordinate Zn are positioned, respectively. The 3D open framework structure of **2** is also characterized by 8M channels along [1 0 0] with NH_4^+ cations situated in them.

Another typical feature of these structures is the presence of the Zn–O–Zn linkages, which is always accompanied by the trigonally coordinated bridging oxygen atoms and the third coordination is always to one P atom. All 3D structures listed in Table 5 have a trigonally coordinated oxygen atoms and infinite Zn–O–Zn chains as a part of the 3D framework. Exceptions are the members of the series with the general formula $M_3[Zn_4O(XO_4)_3](H_2O)_n$ (M=Na, K, Rb, Cs; X=P, As; n=3–6) [41,42] where the bridging oxygen atoms are tetrahedrally coordinated to four Zn cations. It is known that Zn–O–Zn connections with trigonally or tetrahedrally coordinated oxygens are one of the factors that increases the Zn:P ratio [34].

Open framework ZPO structures with Zn:P ratio of 4:3 provide interesting examples of complex topologies (Fig. 7). According to graph theory, the frameworks can be symbolized as graphs with white and black nodes corresponding to the ZnO_4 and PO_4, tetrahedra, respectively [43]. Therefore, the structure can be represented as a graph with nodes symbolizing coordination polyhedra. In accordance with the same theory two nodes of the graph are connected when corresponding tetrahedra share common corners. The representative of the graphs of ZPO structures with Zn:P ratio of 4:3 are shown in Fig. 7. Fig. 7a gives the graph of the layers observed in the 2D framework structure of $(dabcoH)_2[Zn_8(pbc)_6]\cdot 6H_2O$, composed of corner-sharing ZnO_4 and PO_3C tetrahedra (the tetrahedral phosphonate groups) forming an inorganic layer with large 12M rings [44]. Fig. 7b illustrates two members of 2D framework structures: the first is zincophosphate $(C_3H_4N_2)_3[Zn_4(PO_3(OH))(PO_4)_2]$ in which the amine molecule acts as ligand [45,46], and the second is cobalt-doped zincophosphate $(C_3H_4N_2)_3[Zn_{(4-x)}Co_x(PO_3(OH)(PO_4)_2)]$ (x=0.25) [47]. In both compounds an unusual $M_8P_6O_{22}(OH)_2$ (M=Zn, Co) structural unit is present and four such $M_8P_6O_{22}(OH)_2$ structural units are connected together to form a 10M ring. Fig. 7c shows the graph of the 3D open framework structure of $(C_6H_{17}N_3)[Zn_4(OH)(PO_4)_3]$ [40]. Fig. 7a and c graphs correspond to a same topology and the idealized version of these graphs is *cc2-3:4-1* graph shown in Fig. 2.12 in Ref. [43], which contains 12M and 4M rings. It is noteworthy that the M:T ratio is opposite, i.e. it is 3:4 in idealized graph and 4:3 in both structures. Fig. 7d illustrates the graph of orthorhombic potassium tetrazinc phosphate, $KZn_4(PO_4)_3$ [48]. In this structure, basic structural units, which are formed by sharing vertices among two ZnO_4 and two PO_4 tetrahedra, generate ZPO tetrahedral chains along c-axes. The chains are cross-linked to form an open framework with 8M-ring channels along b-axis filled by K atoms. The chain has the *cc2–1:2–1* topology (Fig. 2.3. in Ref. [43]), but M:T ratio is again opposite, i.e. it is 1:2 in idealized graph and 2:1 in the structure. Fig. 7e shows the graph of the series of structures having general formula $M_3[Zn_4O(XO_4)_3](H_2O)_n$ (M=Na, K, Rb, Cs; X=P, As; n=3–6) [41,42]. These structures are based upon the $[Zn_4O(XO_4)_6]$ cluster consisting of an oxocentered OZn_4 tetrahedron linked through common XO_4 groups to form a 3D framework with

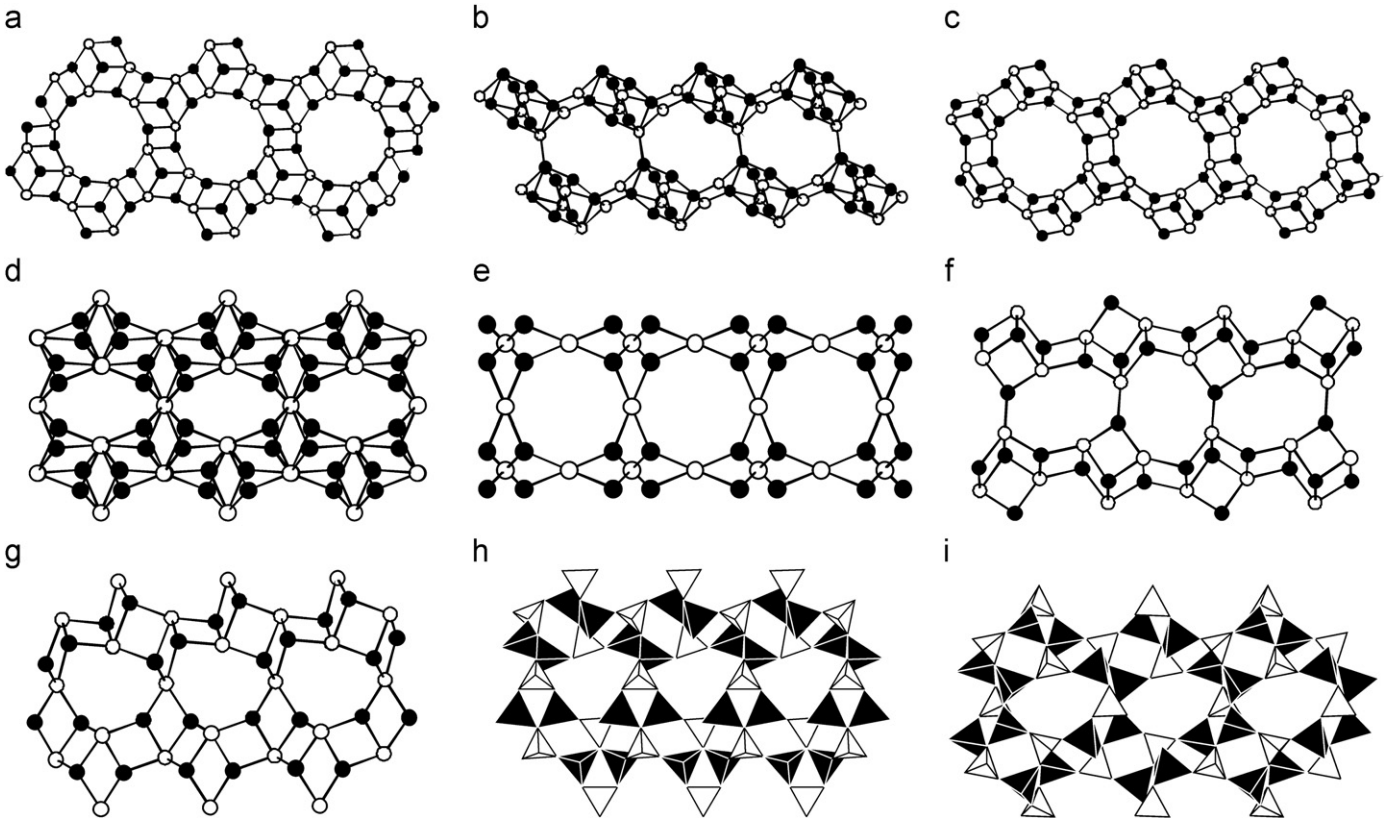

Fig. 7. Nodal representation (black and white nodes symbolize ZnO_4 and PO_4 tetrahedra, respectively) of different layer topologies observed in ZPOs with Zn:P ratio of 4:3 (numbers in parentheses correspond to numbers in Table 5): (a) $(Hdabco)_2[Zn_8(pbc)_6]\cdot 6H_2O$ (2), (b) $(C_3H_4N_2)_3[Zn_{(4-x)}Co_x(PO_3(OH)(PO_4)_2)]$ (x=0.25) and $(C_3H_4N_2)_3[Zn_4(PO_3(OH))(PO_4)_2]$ (3, 4), (c) $(C_6H_{17}N_3)[Zn_4(OH)(PO_4)_3]$ (8), (d) $K[Zn_4(PO_4)_3]$ (17), (e) $M_3[Zn_4O(XO_4)_3](H_2O)n$ (M=Na, K, Rb, Cs; X=P, As; n=3–6) (5, 7), (f) $(C_3H_{10}N)[Zn_4(H_2O)(PO_4)_3]$,$(C_3H_6N_2)[Zn_4(OH)(PO_4)_3]$ (9, 10), $(C_2H_8N)(H_3O)[Zn_4(H_2O)(PO_4)_3]_2\cdot H_2O$ (11), $(NH_4)(H_3O)[Zn_4(PO_4)_3]_2\cdot H_2O$ (16), $(C_2H_8N)[Zn_4(H_2O)(PO_4)_3]$ (12), (g) $(CH_6N)[Zn_4(PO_4)_3]$ (14) and **2** (13). Polyhedral frameworks in (h) **2** (13) and (i) $(CH_6N)[Zn_4(PO_4)_3]$ (14). (For abbreviations and references, see Table 5.)

topology of the primitive cubic lattice regular net [43]. Fig. 7f and g shows the graphs of the several structures having similar structural topologies. The graphs in Fig. 7f and g are consistent to the idealized versions *cc2-3:4-3* and *cc2-3:4–6*, respectively, in Fig. 2.12 in Ref. [43], containing 8M and 4M rings both. The topology *cc2-3:4-3* (Fig. 7f) corresponds to the layers normal to the 8M-ring channels of $(C_3H_{10}N)[Zn_4(H_2O)(PO_4)_3]$ [34], $(C_3H_6N_2)[Zn_4(OH)(PO_4)_3]$ [49], $(C_2H_8N)(H_3O)[Zn_4(H_2O)(PO_4)_3]_2\cdot H_2O$ [39], $(NH_4)(H_3O)[Zn_4(PO_4)_3]_2\cdot H_2O$ [38] and $(C_2H_8N)[Zn_4(H_2O)(PO_4)_3]$ [50], while *cc2-3:4–6* (Fig. 7g) is compatible with the layers observed normal to the 8M-ring channels in $(CH_6N)[Zn_4(PO_4)_3]$ [51] and **2**. Although both correspond to the same *cc2-3:4–6* graph, layers in $(CH_6N)[Zn_4(PO_4)_3]$ [51] and **2** differ by the orientation of tetrahedra relative to the plane of the layers. Figs. 7h and 7i show polyhedral images of these two layers.

The $ZnO_3(NH_3)$ tetrahedra, which were not found in other ZPO structures with Zn:P ratio of 4:3, are an exclusive feature of **2**. Compounds containing both, NH_4^+ ions and coordinated NH_3 molecules, are quite rare and only a small number of them are described so far, e.g. $(NH_4)_2[Zn(CrO_4)_2(NH_3)_2]$ [52], $(NH_4)_2[Cu(CrO_4)_2(NH_3)_2]$ [53], $(NH_4)_2[Cd(CrO_4)_2(NH_3)_2]$ [54] and $(NH_4)[VO(NH_3)PO_4]$ [55]. To our knowledge, **2** is the first 3D ZPO, which incorporates both, the coordinated NH_3 molecule and NH_4^+ cations.

4. Conclusion

Two new ZPOs, bis(ethylenediammonim) *catena*-bis(μ-phosphato)-zincate, $(H_3NCH_2CH_2NH_3)_2[Zn(\mu\text{-}PO_4)_2]$ (**1**), and ammonium ammine-tris(μ-phosphato)-tetrazincate, $(NH_4)[(H_3N)Zn\{(\mu\text{–}PO_4)Zn\}_3]$ (**2**), were synthesized using the hydrothermal method. Their crystal structures and Raman spectra were discussed in detail.

Structural studies showed that the chain structure of **1** contains diprotonated ethylenediammonium cations (H_2en^{2+}) as organic template and represents a new inorganic–organic hybrid compound, whereas **2** is a novel 3D open framework structure with 8M channels. The compound **1**, having the Zn:P ratio of 1:2, is a structure where ZnO_4 and PO_4 tetrahedra are linked to form infinite vertices-shared chains, which are interconnected by H_2en^{2+} cations through a network of hydrogen bonds. The compound **2** with Zn:P ratio 4:3 is characterized by the high tetrahedral atom density (22.42 tetrahedral atoms per 1000 Å^3), and has unique $ZnO_3(NH_3)$ tetrahedral units with NH_4^+ cations situated in 8M channels.

According to Bu and coworkers [34], aluminosilicates could easily vary the framework charge by changing the Si:Al ratio; in this way, they match the charge of cations and/or organic templates with very small modification in the framework topology. On the other hand, the changes in the Zn:P ratio usually results in completely different frameworks, and ZPOs are limited in its ability to vary the framework charge without significant structural changes. The fact that Zn^{2+}, besides four, can also have coordination numbers five and six, or even mixed coordination numbers, like in $Zn_3[PO_3(OH)]_3\cdot 3H_2O$ and $Zn_3(PO_4)_2\cdot H_2O$ [56,57], increases the diversity of new types of ZPO frameworks. Therefore, future studies of metal–phosphate systems with different *M*:P ratios can lead to novel structure types with interesting crystal-chemical properties and understanding how the topology and connectivity depend on experimental conditions

(time, temperature, pH, *M* ionic radii, etc.). This knowledge could be further applied to the similar phosphates, which technical use is based on special physical and chemical characteristics that depend on their crystal structure.

Supporting information available

CCDC 833636 and CSD ID: 423286 contain the supplementary crystallographic data for **1** and **2**, respectively. The crystallographic data for **1** can be obtained free of charge via www.ccdc.cam.ac.uk/data_request/cif, or by emailing data_request@ccdc.cam.ac.uk, or by contacting The Cambridge Crystallographic Data Centre, 12, Union Road, Cambridge CB2 1EZ, UK; fax: +44 1223 336033. Further details of the crystal structure data for **2** may be obtained from Fachinformationszentrum Karlsruhe, 76344 Eggenstein-Leopoldshafen, Germany (fax: (+49)7247–808-666; e-mail: crysdata@fiz-karlsruhe.de, http://www.fiz-karlsruhe.de/request_for_deposited_data.html) on quoting the appropriate CSD number.

Acknowledgments

This work was supported financially by the Ministry for Science and Technological Development of the Republic of Serbia (Grant no. 45007). The authors are thankful to Prof. Dr. Lutz Nasdala for helping with the Raman analysis.

Appendix A. Supporting information

Supplementary data associated with this article can be found in the online version at doi:10.1016/j.jssc.2011.07.030.

References

[1] A.K. Cheetham, G. Férey, T. Loiseau, Angew. Chem. Int. Ed. 38 (1999) 3268–3292.
[2] W.T.A. Harrison, Acta Crystallogr. E57 (2001) i72–i74.
[3] R. Murugavel, A. Choudhury, M.G. Walawalkar, R. Pothiraja, C.N.R. Rao, Chem. Rev. 108 (2008) 3549–3655.
[4] L. Li, D. Sun, G. Tian, X. Song, S. Sun, Cryst. Res. Technol. 44 (2009) 331–335.
[5] Q. Gao, J. Chen, S. Li, R. Xu, J.M. Thomas, M. Light, M.B. Hursthouse, J. Solid State Chem. 127 (1996) 145–150.
[6] E.R. Parnham, R.E. Morris, Acc. Chem. Res. 40 (2007) 1005–1013.
[7] J. Stojanović, T. Đorđević, L.j. Karanović, Acta Crystallogr. C66 (2010) i55–i57.
[8] Oxford Diffraction, CrysAlisPro. Version 1.171.33.31. Oxford Diffraction Ltd, Yarnton, England, 2009.
[9] Z. Otwinowski, W. Minor, Meth. Enzymol. 276 (1997) 307–326.
[10] Z. Otwinowski, D. Borek, W. Majewski, W. Minor, Acta Crystallogr. A59 (2003) 228–234.
[11] A. Altomare, C. Cascarano, C. Giacovazzo, A. Guagliardi, A.G.G. Moliterni, M.C. Burla, G. Polidori, M. Camalli, R. Spagna, SIR97, University of Bari, Italy, 1997.
[12] G.M. Sheldrick, Acta Crystallogr. A64 (2008) 112–122.
[13] L.J. Farrugia, J. Appl. Crystallogr. 32 (1999) 837–838.
[14] E. Dowty, ATOMS for Windows. Version 6.1, A Computer Program, Kingsport, TN, 1999.
[15] R.D. Shannon, Acta Crystallogr. A32 (1976) 751–767.
[16] A.S. Wills, VaList—Bond Valence Calculation and Listing; program available from 〈http://www.ccp14.ac.uk〉, 2009.
[17] I.D. Brown, J. Appl. Crystallogr. 29 (1996) 479–480.
[18] A.L. Spek, Acta Crystallogr. A46 (1990) C34.
[19] Z. Birscak, W.T.A. Harrison, Acta Crystallogr. C54 (1998) 1383–1385.
[20] Q. Gao, A.M. Chippindale, A.R. Cowley, J. Chen, R. Xu, J. Phys. Chem. B101 (1997) 9940–9942.
[21] T.M. Nenoff, W.T.A. Harrison, T.E. Gier, J.C. Calabrese, G.D. Stucky, J. Solid State Chem. 107 (1993) 285–295.
[22] F. Capitelli, B. El Bali, R. Essehli, M. Lachkar, V. Valentini, G. Mattei, J. Taraba, Z. Zak, Z. Kristallogr. 221 (2006) 649–655.
[23] K. Nakamoto, M. Margoshes, R.E. Rundle, J. Am. Chem. Soc. 78 (1955) 6480–6486.
[24] D. Philip, G. Aruldhas, J. Raman Spectrosc. 21 (1990) 211–214.
[25] A. John, D. Philip, A. Khaoulani Idrissi, G. Keresztury, S. Devanarayanan, J. Raman Spectrosc. 31 (2000) 1067–1071.
[26] J. Annamma, D. Philip, K.R. Morgan, S. Devanarayanan, Spectrochim. Acta 56A (2000) 2175–2723.
[27] N.Z. Logar, M. Mrak, V. Kaučič, J. Solid State Chem. 156 (2001) 480–486.
[28] M. Mrak, U. Kolitsch, V. Kaučič, E. Tillmanns, Acta Crystallogr. E58 (2002) i44–i48.
[29] J. Stojanović, T. Đorđević, L.j. Karanović, Acta Crystallogr. C64 (2008) i58–i59.
[30] N. Rajic, N.Z. Logar, A. Golobic, V. Kaucic, J. Phys. Chem. Solids 64 (2003) 1097–1103.
[31] D.S. Wragg, B.L. Ouay, A.M. Beale, M.G. O'Brien, A.M.Z. Slawin, J.E. Warren, T.J. Prior, R.E. Morris, J. Solid State Chem. 183 (2010) 1625–1631.
[32] A.A. Ayi, S. Neeraja, A. Choudhurya, S. Natarajana, C.N.R. Raoa, J. Phys. Chem. Solids 62 (2001) 1481–1491.
[33] P.A. Boudjada, D. Tranqui, J.C. Guitel, Acta Crystallogr. B36 (1980) 1176–1178.
[34] X. Bu, P. Feng, G.D. Stucky, J. Solid State Chem. 125 (1996) 243–248.
[35] Z. Chen, Y. Zhou, L. Weng, D. Zhao, Cryst. Growth Des. 8 (2008) 4045–4053.
[36] W.T.A. Harrison, M.L.F. Phillips, A.V. Chavez, T.M. Nenoff, J. Mater. Chem. 9 (1999) 3087–3092.
[37] W.H. Meier, D.H. Olson, Ch. Baerlocher, Atlas of Zeolite Structure Types, Elsevier, Boston, USA, 1996.
[38] S. Neeraj, C.N.R. Rao, A.K. Cheetham, J. Mater. Chem. 14 (2004) 814–820.
[39] S. Neeraj, A.K. Cheetham, Chem. Commun. 2002 (2002) 1738–1739.
[40] K.O. Kongshaug, H. Fjellvåg, K.P. Lillerud, Micropor. Mesopor. Mater. 39 (2000) 341–350.
[41] W.T.A. Harrison, R.W. Broach, R.L. Bedard, T.E. Gier, X. Bu, G.D. Stucky, Chem. Mater. 8 (1996) 691–700.
[42] W.T.A. Harrison, M.L.F. Phillips, X.H. Bu, Micropor. Mesopor. Mater. 39 (2000) 359–365.
[43] S.V. Krivovichev, Structural Crystallography of Inorganic Oxysalts, Oxford University Press, Oxford, 2008.
[44] J.-T. Li, D.-K. Cao, B. Liu, Y-Zh.Li, L-M. Zheng, Cryst. Growth Des. 8 (2008) 2950–2953.
[45] A. Cui, Y. Yao, Chem. Lett. 30 (2001) 1148–1149.
[46] Y. Xing, Y. Liu, Z. Shi, P. Zhang, Y. Fu, C. Cheng, W. Pang, J. Solid State Chem. 163 (2002) 364–368.
[47] L. Liu, H. Meng, G. Li, Y. Cui, H. Ding, Y. Xing, W. Pang, Mater. Lett. 59 (2005) 1752–1755.
[48] M.T. Averbuch-Pouchot, A. Durif, Acta Crystallogr. B35 (1979) 151–152.
[49] S. Natarajan, S. Neeraj, C.N.R. Rao, Solid State Sci. 2 (2000) 87–98.
[50] T. Song, M.B. Hursthouse, J. Chen, J. Xu, K.M.A. Malik, R.H. Jones, R. Xu, J.M. Thomas, Adv. Mater. 6 (1994) 679–680.
[51] Y. Song, P.Y. Zavalij, M.S. Whittingham, J. Mater. Chem. 13 (2003) 1936–1941.
[52] M. Harel, C. Knobler, J.D. McCullough, Inorg. Chem. 8 (1969) 11–13.
[53] B.M. Gatehouse, L.W. Guddat, Acta Crystallogr. C43 (1987) 1445–1447.
[54] H. Headlam, M.A. Hitchman, H. Stratemeier, J.M.M. Smits, P.T. Beurskens, E. de Boer, G. Janssen, B.M. Gatehouse, G.B. Deacon, G.N. Ward, M.J. Riley, D. Wang, Inorg. Chem. 34 (1995) 5516–5523.
[55] D. Fratzky, H. Worzala, T. Goetze, M. Meisel, Acta Crystallogr. C55 (1999) 156–157.
[56] A. Riou, Y. Cudennec, Y. Gerault, Acta Crystallogr. C43 (1987) 194–197.
[57] A. Riou, Y. Cudennec, Y. Gerault, Rev. Chim. Miner. 23 (1986) 810–818.